JPE 11-2-11

Maximum Efficiency Point Tracking Algorithm Using Oxygen Access Ratio Control for Fuel Cell Systems

Min-Ho Jang†, Jae-Moon Lee*, Jong-Hoon Kim**, Jong-Hu Park***, and Bo-Hyung Cho**

†** Dept. of Electrical and Electronics Eng., Seoul National University, Seoul, Korea
* Fuel Cell Vehicle Team, Hyundai Motor Company, Yongin, Korea
*** Dept. of Electrical and Electronics Eng., Soongsil University, Seoul, Korea

Abstract

The air flow supplied to a fuel cell system is one of the most significant factors in determining fuel efficiency. The conventional method of controlling the air flow is to fix the oxygen supply at an estimated constant rate for optimal efficiency. However, the actual optimal point can deviated from the pre-set value due to temperature, load conditions and so on. In this paper, the maximum efficiency point tracking (MEPT) algorithm is proposed for finding the optimal air supply rate in real time to maximize the net-power generation of fuel cell systems. The fixed step MEPT algorithm has slow dynamics, thus it affects the overall efficiency. As a result, the variable step MEPT algorithm is proposed to compensate for this problem instead of a fixed one. The complete small signal model of a PEM Fuel cell system is developed to perform a stability analysis and to present a design guideline. For a design example, a 1kW PEM fuel cell system with a DSP 56F807 (Motorola Inc) was built and tested using the proposed MEPT algorithm. This control algorithm is very effective for a soft current change load like a grid connected system or a hybrid electric vehicle system with a secondary energy source.

Key Words: Air flow control, Fuel cell system, Fuel efficiency, Maximum efficiency point, MEPT algorithm

I. INTRODUCTION

Fuel cells are drawing the attention of the governments all over the world, because they have a lot of excellent characteristics such as high efficiency, environment friendliness and so on[1]-[4]. Especially, proton exchange membrane (PEM) fuel cells have high power density and efficiency. Also, they operate at a low temperature and start up rapidly when compared to other fuel cells [5].

A fuel cell (FC) system has a movable operating point according to the output current of the FC, which determines the FC stack voltage represented as a voltage source. Since the consumption rate of hydrogen fuel is proportional to the output current[6], [7], the operating point determines the amount of fuel used. The controller in a FC system adjusts the compressor operation in order to regulate the humidified air supply for the required power generation. Fig. 1 shows an entire FC system diagram displaying the controlling parameter W_{air_ref} and the process.

The conventional method of controlling the air flow is to fix the oxygen supply at a constant rate as required for the FC reaction. By the rule of thumb, the oxygen access ratio (λ_{O2}) is typically recommended to be pre-set to the value 2[7]-[12]. However, the actual optimal point can deviate from the pre-set value due to various operating conditions such as very light or heavy load situations. In fact, the experimental measurements of the FC system in this paper show that the optimal supply rate varies very sensitively according to given operating condition changes, staying far away from a pre-set value λ_{O2}, thus degrading the power generation performance. To compensate for this problem, recent literature has proposed a λ_{O2} tracking control method using a linearized model[13]-[16]. However, the maximum ratio varies according to FC stack aging and environmental factors such as temperature and humidity variation directly affect the air pressure[17]. Also, an exact linearized re-model is neccessary to apply the model-based tracking algorithm to another FC system. Hence an algorithm which maximizes the net power by supplying an amount of air for optimal control without any effects from those conditions must be developed[18].

In this paper, a maximum efficiency point tracking (MEPT) algorithm based on the perturbation and observation (P&O) method is proposed for finding the optimal air supply rate to maximize the net-power generation of an FC system. A MEPT algorithm using a 'variable' step size is proposed, and its performance is compared with a fixed step MEPT

Manuscript received Jul. 19, 2010; revised Jan. 10, 2011
† Corresponding Author: jang10000ho@hotmail.com
Tel: +82-2-880-1785, Fax: +82-2-878-1452, Seoul Nat'l University
* Fuel Cell Vehicle Team, Hyundai Motor Company, Korea
** Dept. of Electrical and Electronics Eng., Seoul Nat'l University, Korea
*** Dept. of Electrical and Electronics Eng., Soogsil University, Korea

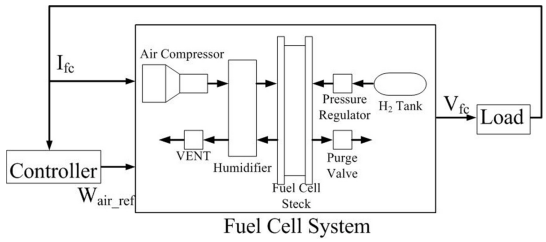

Fig. 1. PEM fuel cell system diagram.

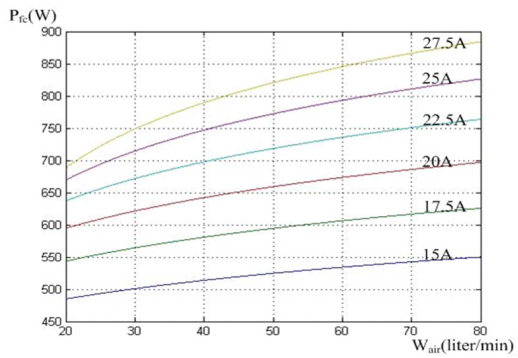

Fig. 2. Relation between Output power and the air supply in 1kW PEMFC power system.

algorithm. A MEPT algorithm has a performance trade-off between the sampling period and the step size for stable operation, therefore the dynamic response analysis of an FC system including an air compressor should be considered when designing these two factors.

This paper is organized as follows. In Section II, the fundamental concept of a MEPT algorithm is derived. Also, a variable step MEPT algorithm is proposed. In Section III, the stability of the proposed MEPT algorithm is verified through small signal modeling and a design guideline is suggested. The dynamic models for small signal modeling used in this paper are from [19]. For verification of the proposed MEPT algorithm, a 1kW FC system with a DSP56F807 has been built and tested as detailed in Section IV. Finally, the conclusions of this paper are presented in Section V.

II. MEPT Algorithm

As the amount of air provided to the FC increases, the partial pressure at the cathode also rises. Then, the output voltage increases with the log scale as shown in eq. (1) (See Fig. 2. The output voltage rise implies that the voltage drop in the FC stack decreases, which leads to a higher output power from an equal amount of hydrogen fuel when compared to that with a lower air pressure. Therefore, it is desirable for the amount of air provided to the cathode to be set higher than the amount of the oxygen required for the fuel reaction.

$$\begin{aligned} v_{fc} &= V_{OC} + V_{an,H_2} + V_{ca,O_2} \\ &= V_{OC} + \log(p_{an,H_2}) \times K_{p_{H_2}} \times (T_{fc} - 298.15) \\ &+ \log(p_{ca,O_2}) \times K_{p_{O_2}} \times (T_{fc} - 298.15) \end{aligned} \quad (1)$$

where p_{an,H_2} is the partial pressure of the hydrogen anode
p_{ca,O_2} is the partial pressure of the oxygen cathode
T_{fc} is the temperature of the fuel cell
$K_{p_{H_2}}$ and $K_{p_{O_2}}$ are the OCV constants of the channel.

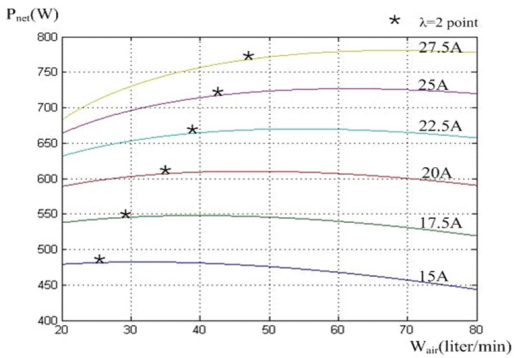

Fig. 3. Relation between Net power and the air supply in 1kW PEMFC power system.

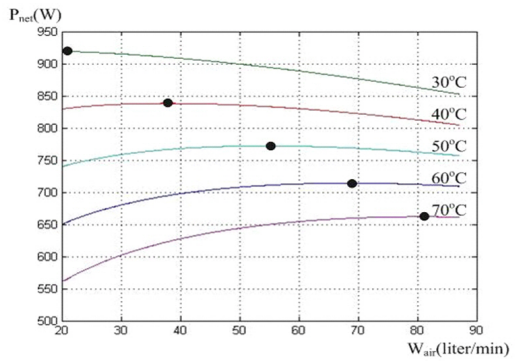

Fig. 4. Simulation of net power according to the fuel cell temperature change ($I_{fc} = 25A$).

However, there exists some loss caused by the air compressor when providing the air supply to the FC. The net power can be obtained by subtracting the power loss in the air compressor from the generated power of the FC system. When the air pump speed increases in order to enhance the air (Oxygen) flow, the consumed power in the compressor also increases. Consequently, there exists a trade-off between the generated system power and the peripheral power consumption. This means that it is necessary to control the air compressor for optimal operation of the FC stack.

The conventional method for controlling the air flow is to fix the oxygen supply to a constant oxygen access ratio (λ_{O2}) based on how many required for the FC reaction. This method contributes to a fast response to current changes by quickly deciding the amount of air to be supplied instantaneously. However, the actual optimal point can deviated from the pre-set value due to various operating condition such as very light or heavy load situations. The commonly used oxygen access ratio (λ_{O2}) value of 2 is used as the conventional algorithm for comparison with the proposed algorithm in this paper. Fig. 3 shows that the pre-set value of 2 has the best performance under light loads but it is not good under heavy loads. Furthermore, the maximum rate changes according to FC stack aging and environmental factors such as temperature and humidity variations directly affecting the air pressure (see Fig. 4). Hence, an algorithm which maximizes the net power by supplying an amount of air for optimal control without being effected by those conditions must be developed. In this paper, the maximum efficiency point tracking (MEPT) algorithm is proposed for finding the optimal air supply rate

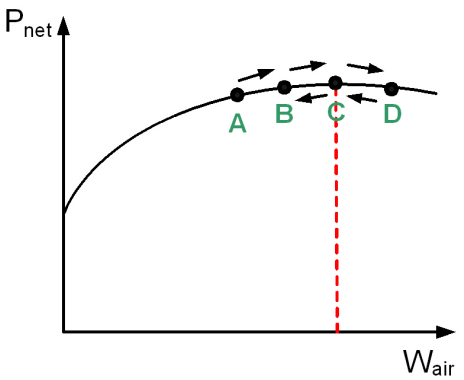

Fig. 5. Operation of the fixed step MEPT Algorithm.

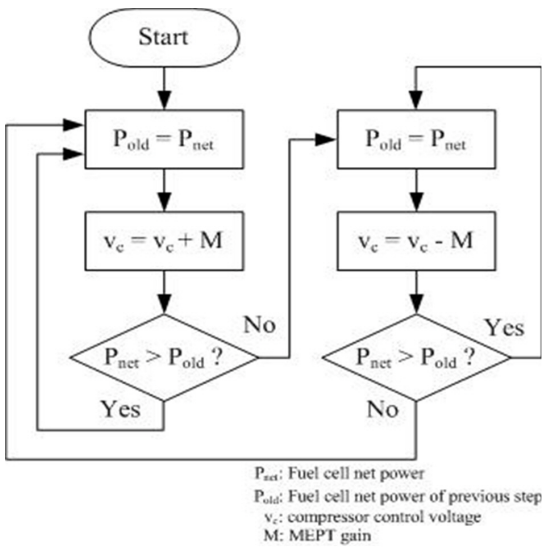

Fig. 6. Fixed step MEPT Algorithm flow chart.

to maximize the net-power generation of FC systems.

A. *Fixed step MEPT Algorithm*

The most basic MEPT algorithm suggested in this paper is used for tracking the optimal efficiency point using a fixed step size (M). This tracking operation is shown in Fig. 5. The MEPT algorithm changes the amount of air supplied to the FC and then compares the current net power (P_{net}) with the previous one (P_{old}). It then alters the amount of air supplied to reach the greatest power-generation point. The amount of air supply is controlled by the air compressor reference voltage (v_c). A flow chart of the fixed step MEPT algorithm is shown in Fig. 6.

B. *Variable step MEPT Algorithm*

The fixed step algorithm has a slow dynamic in MEPT, especially when the initial operating point is far away from the optimal point, which affects the overall efficiency. Therefore, the variable step MEPT algorithm is proposed to compensate for this problem instead of the fixed one (see Fig. 7). The fundamental operation of the variable step MEPT algorithm is based on the previous one. As a result, the steady state operation is same as with the fixed step MEPT algorithm. However, the variable step MEPT algorithm increases the

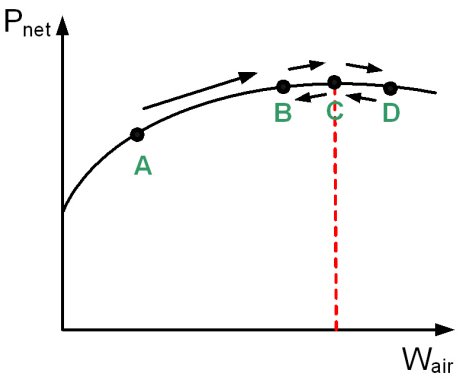

Fig. 7. Operation of the variable step MEPT Algorithm.

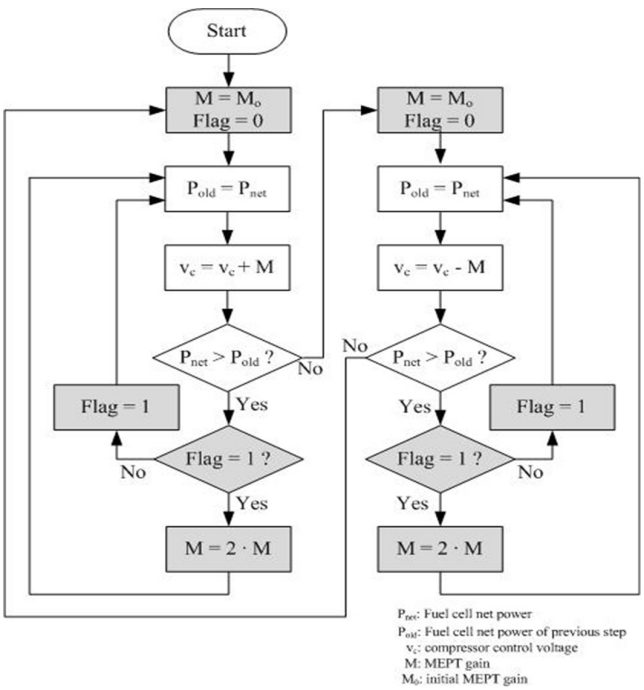

Fig. 8. Variable step MEPT Algorithm flow chart.

step size when the reference of the MEPT controller moves unidirectional for more than 2 sampling cycles, since it is assumed that the operating position is far from the maximum peak point. In this procedure, the parameter 'Flag' is used to determine the previous reference's direction. On the other hand, the MEPT controller resets the step size 'M_0' (the same as the fixed step MEPT algorithm gain) when current net power is smaller than the previous one. This operation is marked with a gray color in flow chart (see Fig. 8).

III. Dynamic Analysis of the MEPT Algorithm

The operation of the proposed MEPT algorithm is based on the perturbation and observation (P&O) method which compares the net power before-and-after the air pressure reference update. The sampling period for the measurement of the net power should be long enough to obtain stable data from the system when the air supply changes. Fig. 9 shows the transient response of the stack and the net power when the air compressor reference is step-changed. The dissipated power of the compressor increases faster than the power generated in the FC stack. Therefore, the net power in the graph shows

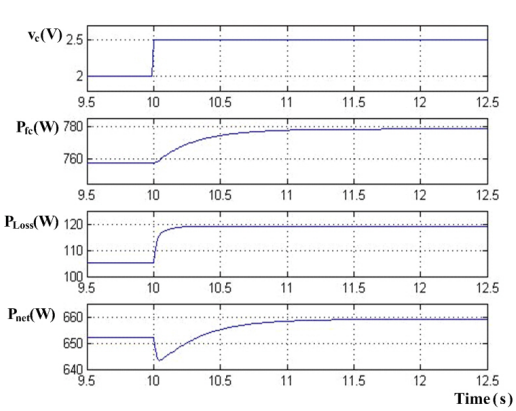

(a) Air compressor reference step up.

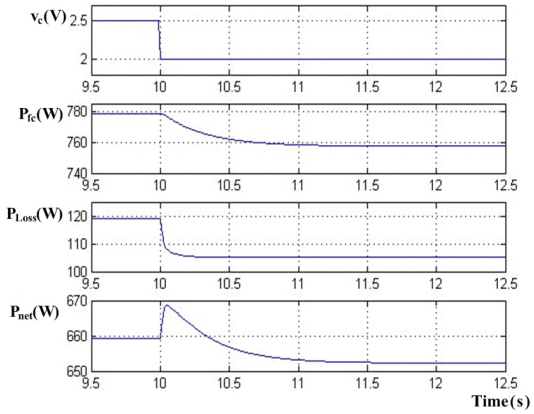

(b) Air compressor reference step down.

Fig. 9. Dynamic analysis of fuel cell system.

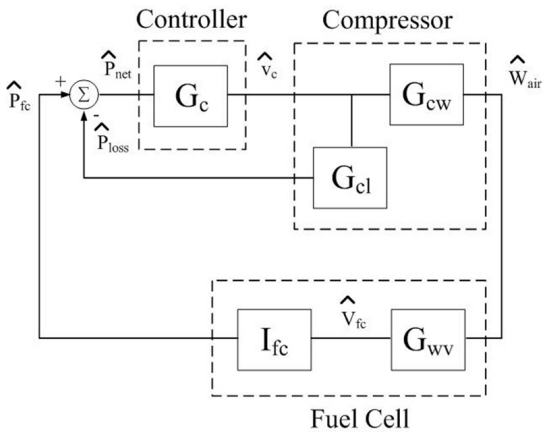

Fig. 10. Control block diagram of the FC power system for the proposed MEPT algorithm.

a decrease when the compressor reference increases stepwise. Therefore, an excessively high sampling frequency for the measurement of the algorithm results in an incorrect decision. The MEPT algorithm has a performance trade-off between the sampling period and the step size for stable operation. Therefore, the dynamic response analysis of the FC system including the air compressor should be considered when designing these two factors. Fig. 10 shows the small-signal transfer function model of an FC system with the MEPT algorithm.

A. *Fuel cell transfer function*

Using eq. (1), the transfer function from the partial pressure of the cathode to the FC output voltage is derived by the perturbation and linearization technique as follows:

$$\frac{\hat{v}_{fc}}{\hat{p}_{O_2}} = 8.75 \times K_{p_{O_2}} \times (T_{fc} - 298.15). \tag{2}$$

Since oxygen makes up 21% of the total air supply, the transfer function from the air flow of the compressor to the partial pressure of the cathode can be easily derived by multiplying the transfer function of the oxygen flow to the partial pressure of the cathode by 0.21.

$$\begin{aligned} \frac{\hat{p}_{O_2}}{\hat{w}_{air}} &= \frac{\hat{w}_{O_2}}{\hat{w}_{air}} \cdot \frac{\hat{p}_{O_2}}{\hat{w}_{O_2}} \\ &= 0.21 \cdot \frac{1}{k_{ca}} \cdot \frac{1}{(1 + \frac{s}{A_{O_2} \cdot k_{ca}})} \end{aligned} \tag{3}$$

where $A_{O_2} = \frac{R_{O_2} \cdot T_{fc}}{V_{ca}}$

R_{O_2}: gas constants of oxygen (J/mol·K)

V_{ca}: cathode channel volume (m^3)

k_{ca}: orifice constant.

Considering eq. (2) and (3), the total open-loop transfer function of the FC system G_{wv} is derived as follows:

$$\begin{aligned} G_{wv} = \frac{\hat{v}_{fc}}{\hat{w}_{air}} &= \frac{\hat{p}_{O_2}}{\hat{w}_{air}} \cdot \frac{\hat{v}_{fc}}{\hat{p}_{O_2}} \\ &= 1.84 \times K_{p_{O_2}} \times (T_{fc} - 298.15) \times \frac{1}{k_{ca}} \cdot \frac{1}{(1 + \frac{s}{A_{O_2} \cdot k_{ca}})}. \end{aligned} \tag{4}$$

B. *Air compressor transfer function*

The dynamic response of the air compressor is almost ten times faster than that of the FC system derived from the previous dynamic analysis. An approximation assuming that the transfer function of the air compressor is constant is allowed due to a fast dynamic response with a negligible error when the control loop design for the MEPT algorithm is used.

$$\begin{aligned} G_{cw} &= \frac{\hat{w}_{cp}}{\hat{v}_c} = K_w \\ G_{cl} &= \frac{\hat{P}_{Loss}}{\hat{v}_c} = K_l. \end{aligned} \tag{5}$$

C. *Total transfer function (without the MEPT algorithm)*

The total system transfer function, except the MEPT algorithm control loop using the previous transfer functions, is as

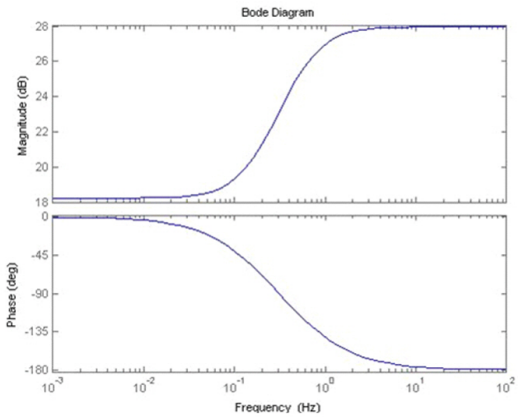

(a) Light load condition at $I_{fc} = 10A$ (zero < pole).

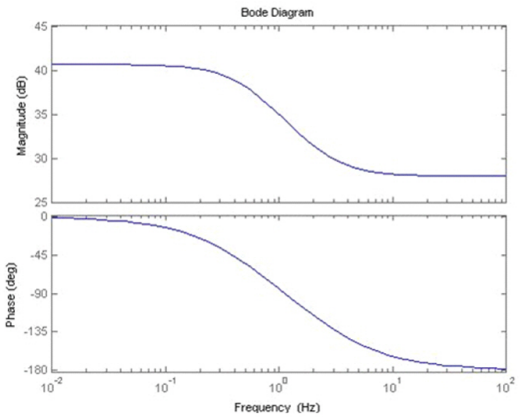

(b) Heavy load condition at $I_{fc} = 40A$ (zero > pole).

Fig. 11. Total transfer function without MEPT algorithm. $\left(\frac{\hat{P}_{net}}{\hat{v}_c}\right)$

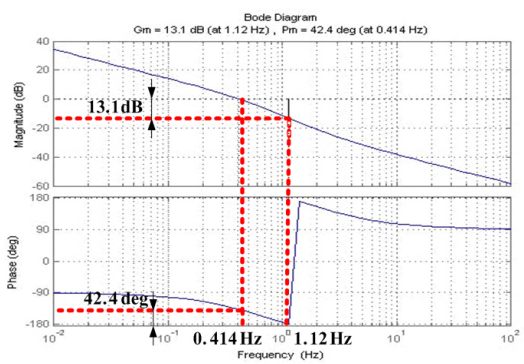

(a) Light load condition at $I_{fc} = 10A$ (zero < pole).

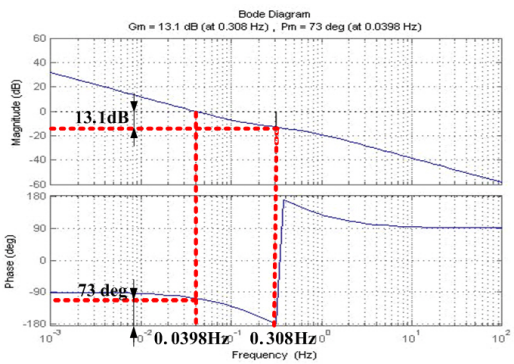

(b) Heavy load condition at $I_{fc} = 40A$ (zero > pole).

Fig. 12. Phase margin of MEPT algorithm (T_{mept}).

follows:

$$\frac{\hat{P}_{net}}{\hat{v}_c} = I_{fc} \cdot G_{wv} \cdot G_{cw} - G_{cl} = \left(\frac{K_{fc} \cdot I_{fc}}{k_{ca}} - K_l\right) \cdot \frac{1 - \frac{s}{w_z}}{1 + \frac{s}{w_p}} \quad (6)$$

where $w_z = \left(\frac{K_{fc} \cdot I_{fc}}{K_l \cdot k_{ca}} - 1\right) \cdot A_{O_2} \cdot k_{ca}$
$w_p = A_{O_2} \cdot k_{ca}$

As shown in eq. (6), the transfer function has a left half-plane pole and a right half-plane (RHP) zero. Since the RHP zero moves according to the FC's output current and may lie within the range which affects the MEPT algorithm's behavior, the dynamic response should be carefully analyzed under heavy and light load conditions. Depending on the relative location of the pole and zero, the transfer function has differerent bode plots, which are shown in Fig. 11.

D. MEPT controller transfer function

The mathematical relation, under steady-state operation, of the two proposed MEPT algorithms can be established as follows:

$$v_c(k+1) = v_c(k) + M\text{sgn}\left(\frac{\Delta P_{net}}{\Delta v_c}\right) \quad (7)$$

where M is the variation step size of the air compressor reference.

This relation can be expressed with an integrator including the sampling time of the control command update as follows[20]:

$$G_c = \frac{\hat{v}_c}{\hat{P}_{net}} = \frac{M}{T_s \cdot s} \quad (8)$$

where T_s : sampling time of the controller.

E. Design of the MEPT algorithm

Using the eq. (6) and (8), the closed loop gain of the total system including the MEPT control is derived as eq. (9). The loop gain also has different dynamic characteristics according to the relationship between the pole and the zero.

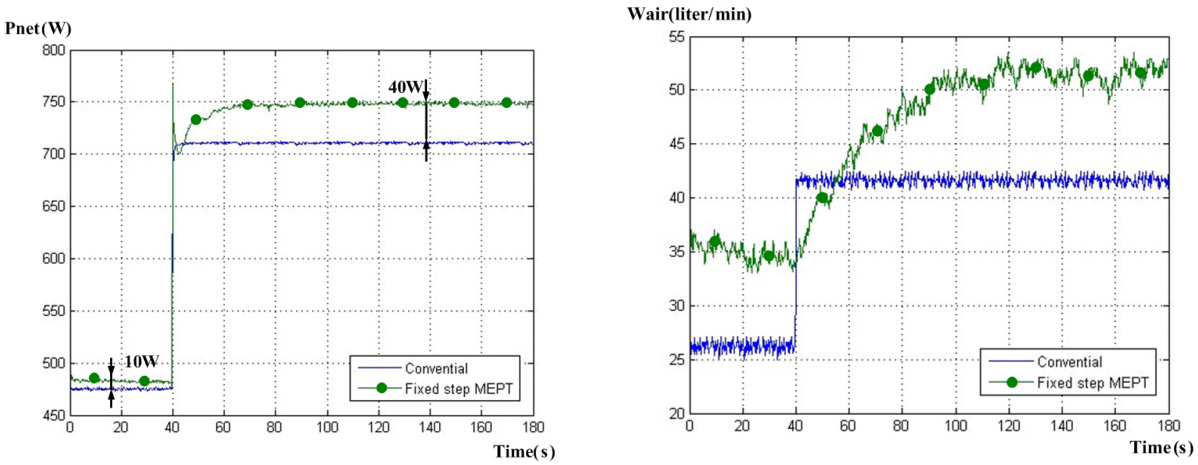

(a) Fuel cell system net power. (b) Mass of air flow by air compressor.

Fig. 13. Comparison of the experimental results between a conventional algorithm and the fixed step MEPT algorithm (15A to 25A load condition).

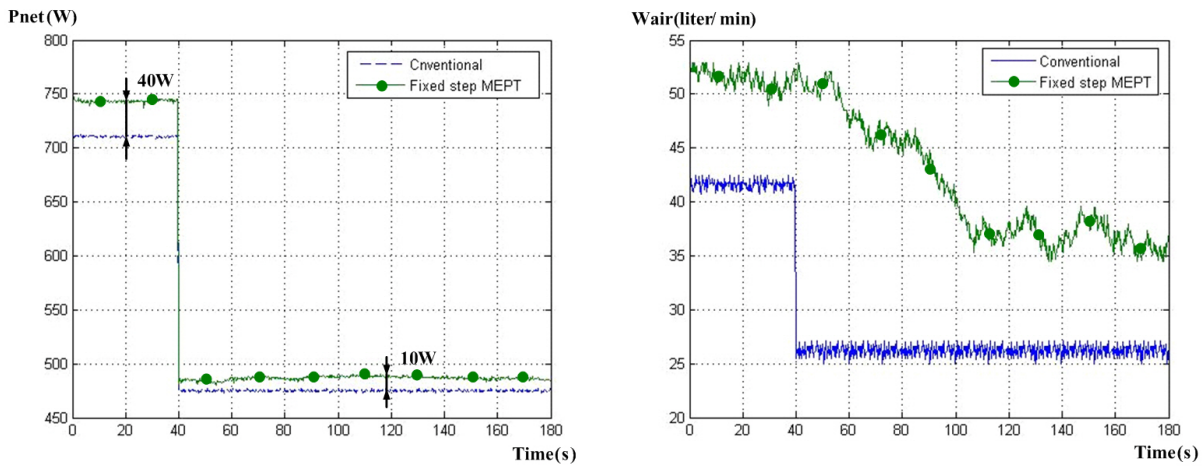

(a) Fuel cell system net power. (b) Mass of air flow by air compressor.

Fig. 14. Comparison of the experimental results between a conventional algorithm and the fixed step MEPT algorithm (25A to 15A load condition).

$$T_{mept} = \frac{\hat{P}_{net}}{\hat{v}_c} \cdot \frac{\hat{v}_c}{\hat{P}_{net}} = \left(\frac{K_{fc} \cdot I_{fc}}{k_{ca}} - K_l \right) \cdot \frac{M}{T_s} \cdot \frac{1}{s} \cdot \frac{1 - \frac{s}{w_z}}{1 + \frac{s}{w_p}} \quad (9)$$

As shown in Fig.11., the zero dominantly affects the dynamic response and the stability when the right half-plane zero is located lower than the left half-plane pole in the bode plot, otherwise the pole dominates. For a phase margin that is greater than 45°, the following requirements should be satisfied [21],[22]:

$$\frac{M}{T_s} < \frac{A_{O_2} \cdot k_{ca}}{K_l} (\text{for } w_z < w_p)$$
$$\frac{M}{T_s} < \frac{A_{O_2} \cdot k_{ca}^2}{K_{fc} \cdot I_{fc} - K_l \cdot k_{ca}} (\text{for } w_z < w_p) \quad (10)$$

In this paper, the sampling time was 1 sec. in order to obtain a fast dynamic response. This leads to selecting 0.03 for the air-compressor step parameter M from eq. (10). The total system closed loop response is presented as shown in Fig. 12. The loop gain has about a 45° phase margin under the heavy load condition for control stability.

IV. Experimental Results

In this paper, a 1kW PEMFC system is used to verify the MEPT algorithm. The system's output current and voltage operate between 0A(45V) to 40A(25V). A 16 bit digital signal processor 56F807 (Motorola Inc) is used as a system controller for the MEPT algorithm.

The experimental results with the FC system compare the performance of the two algorithms, which are the conventional control with a constant oxygen access ratio ($\lambda_{O2} = 2$) and the fixed step MEPT. Fig. 13 shows the results of a 15A to 25A step up load current and Fig. 14 shows a 25A to 15A step down load current by electric load. The results show that the MEPT algorithm produces a higher net power than the conventional one by 10W at the 15A load condition

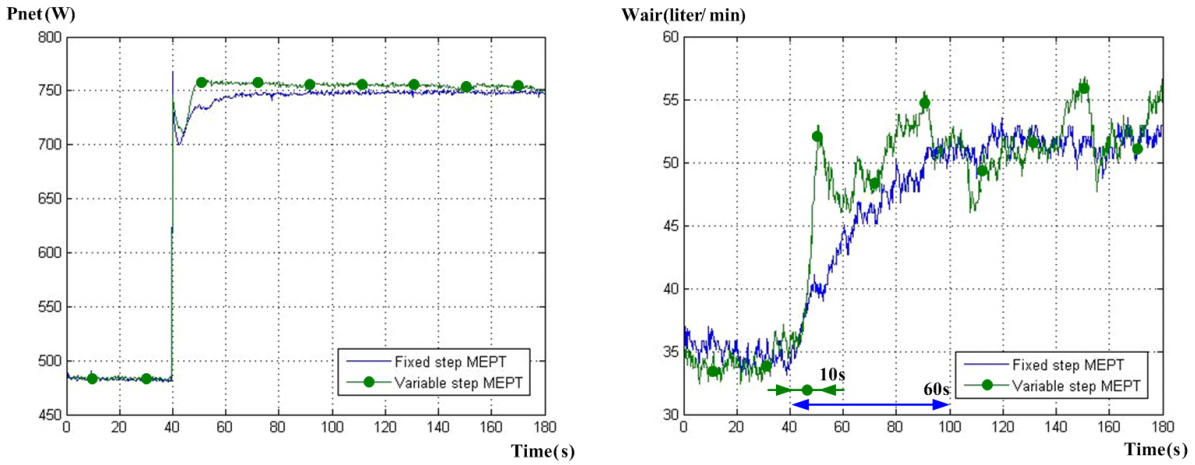

(a) Fuel cell system net power. (b) Mass of air flow by air compressor.

Fig. 15. Comparison of the experimental results between the fixed step MEPT and the variable step MEPT algorithm (15A to 25A load condition).

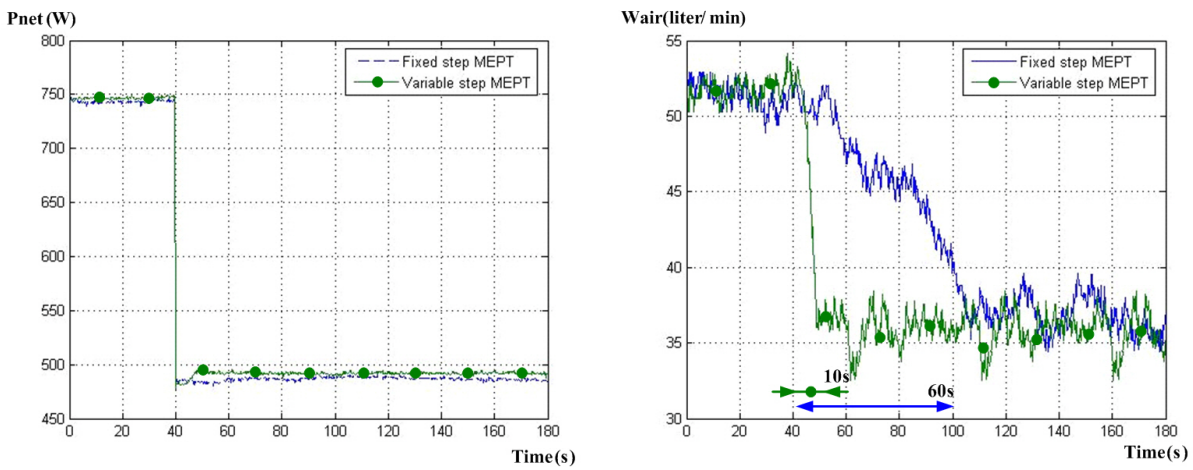

(a) Fuel cell system net power. (b) Mass of air flow by air compressor.

Fig. 16. Comparison of the experimental results between the fixed step MEPT and the variable step MEPT algorithm (25A to 15A load condition).

and by 40W at the 25A load condition. The net power and the amount of air supplied measured under the same load condition as the previous experiment is presented in Fig. 15 and 16 for a performance comparison between the fixed step MEPT algorithm and the proposed variable step MEPT algorithm. The fundamental operation of the variable MEPT algorithm is the same as that of the fixed step MEPT algorithm, so the steady state net power is same as the previous one. At a given load change, the results show that the variable step MEPT algorithm has a faster tracking speed with a settling time of 10s, compared to the fixed step MEPT algorithm with a settling time of 60s.

V. Conclusions

In this paper, optimal oxygen ratio tracking algorithms with a fixed step size and a variable step size are proposed for fuel cell systems. The variable step MEPT algorithm automatically adjusts the step size based on the distance between the maximal efficiency point and the current operating point of the FC. Through small signal modeling, it is verified that the proposed algorithm is stable for all operating cases. For verification of the proposed algorithm, a 1kW fuel cell system with a DSP 56F807 was built and tested. The result shows that the proposed algorithm produces a higher net power than the conventional one by 10W at a 15A load condition and by 40W at a 25A load condition. Furthermore, the variable step MEPT algorithm has a faster tracking speed with a settling time of 10s, compared to the fixed step MEPT algorithm with a settling time of 60s. Since there exists the chance of optimizing the way to change the step size of a MEPT algorithm, the proposed variable step algorithm in this paper suggests a direction for improving the response.

Acknowledgment

This work was supported by the ERC program of MOST/KOSEF (Grant No. R11-2002-102-00000-0) and the Human Resources Development Project of the Korea Institute of Energy Technology Evaluation and Planning (KETEP)

funded by the Ministry of Knowledge Economy, Republic of Korea (Grant No. 20104010100610).

REFERENCES

[1] M. W. Ellis, M. R. Von Spakovsky, and D. J. Nelson, "Fuel cell systems: efficient, flexible energy conversion for the 21st century," in *Proc. IEEE*, Vol. 89, No. 12, pp. 1808-1818, Dec. 2001.

[2] Y. Kishinevsky and S. Zelingher, "Coming clean with fuel cells," *IEEE Power & Energy Magazine*, Vol. 1, No. 6, pp. 20-25, Nov./Dec. 2003.

[3] S. S. Williamson, S. C. Rimmalapudi, and A. Emadi, "Electrical modeling of renewable energy sources and energy storage devices," *Journal of Power Electronics*, Vol. 4, No. 2, pp. 117-126, Apr. 2004.

[4] J.-G. Lim, S.-K. Chung, "Implementation of a fuel cell dynamic simulator," *Journal of Power Electronics*, Vol. 7, No. 4, pp. 336-342, Oct. 2007.

[5] J. K. Shin, "Performance analysis and optimization of control strategy for fuel cell hybrid vehicle using battery and ultra capacitor," Dissertation, Department of Electrical Engineering, Seoul National University, 2005.

[6] A. J. del Real, A. Arce, and C. Bordons, "Development and experimental validation of a PEM fuel cell dynamic model," *Journal of Power Sources*, Vol. 173, No.1, pp. 310-324, Nov. 2007.

[7] J. T. Pukrushpan, A. G. Stefanopoulou, and H. Peng, "Control of fuel cell breathing," *Control System Magazine,* Vol.24, No. 2, pp. 30-46, Apr. 2004.

[8] A. Vahlidi, A.G. Stefanopoulou, and H. Peng, "Current management in a hybrid fuel cell power system: A model-predictive control approack," *IEEE Trans. Control Syst. Technol.*, Vol. 14, No.6, pp. 1047-1057, Nov. 2006.

[9] Z. Zhong, H. Huo, X. Zhu, G. Cao, and Y. Ren, "Adaptive maximum power point tracking control of fuel cell power plants," *Journal of Power Sources*, Vol. 176, No. 1, pp. 259-269, 2008.

[10] J. T. Pukrushpan, A. G. Stefanopoulou, and H. Peng, "Modeling and control for PEM fuel cell stack system," *American Control Conference*, Vol. 4, pp. 3117-3122, 2002.

[11] K. W. Suh and A. G. Stefanopulou, "Performance limitations of air flow control in power-autonomous fuel cell systems," *IEEE Trans. Control Syst. Technol.*, Vol. 15, No. 3, pp. 465-473, May 2007.

[12] C. Bordons, A. Arce, and A. J. del Real, "Constrained predictive control strategies for PEM fuel cells," *American Control Conference*,pp. 6088-6093, Dec. 2006.

[13] C. Ramos, A. Romero, R. Giral, and L. Martinez-Salamero, "Maximum power point tracking strategy for fuel cell power systems," in *Proc. IEEE ISIE*, pp. 2613-2618, 2007.

[14] J. Zhang, G. Liu, W. Yu, and M. Ouyang, "Adaptive control of the air flow of a PEM fuel cell system," *Journal of Power Sources*, Vol. 179, No. 2, pp. 649-659, May 2008.

[15] C. A. Ramos-Paja, C. Bordons, A. Romero, R. Giral, and L. Martinez-Salamero, "Minimum fuel consumption strategy for PEM fuel cells," *IEEE Trans. Ind. Eletron.*, Vol. 56, No. 3, pp. 685-696, Mar. 2009.

[16] C. A. Ramos-Paja, R. Giral, L. Martinez-Salamero, J. Romano, A. Romero, and G. Spagnuolo, "A PEM fuel cell model featuring oxygen excess ratio estimation and power electronics interaction," *IEEE Trans. Ind. Eletron.*, Vol. 57, No. 6, pp. 1914-1924, Jun. 2010.

[17] Y. A. Chang and S. J. Moura, "Air flow control in fuel cell systems: an extremum seeking approach," *American Control Conference*, pp. 1052-1059, 2009.

[18] A. Giustiniani, G. Petrone, C. Pianese, M. Sorrentino, G. Spangnuolo, and M. Vitelli, "PEM fuel cells control by means of the perturb and observe technique," in *Proc. IEEE IECON*, pp. 4349-4354, 2006.

[19] J.-M. Lee and B.-H. Cho, "A dynamic model of a PEM fuel cell system," *Applied Power Electronic Conference and Exposition*, pp. 720, 2009.

[20] H.-S. Bae, J.-H. Park, B.-H. Cho, and G.-J. Yu, "New MPPT control strategy for two-stage grid-connected photovoltaic power conditioning system," *Journal of Power Electronics*, Vol. 7, No. 2, pp. 174-180, Apr. 2007.

[21] P. Huynh, "Analysis and Design of Microprocessor-Controlled Peak-Power Tracking System". Ph. D. Dissertion, VPEC, 1992.

[22] J.-H. Lee, H.-S. Bae, and B.-H. Cho, "Advanced incremental conductance MPPT algorithm with a variable step size," in *Proc. EPE*, pp. 603-607, 2006.

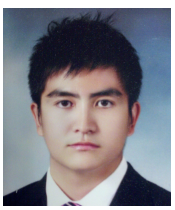

Min-Ho Jang was born in Seoul, Republic of Korea in 1985. He received his B.S. and M.S. in Electrical Engineering from Seoul National University (SNU), Seoul, Republic of Korea, in 2007 and 2010, respectively. He is currently a Researcher at Hyundai Heavy Industries, Republic of Korea. His main research interests include power electronics, the modeling, analysis and control of electric vehicle power systems and fuel cell systems.

Jae-Moon Lee was born in Seoul, Republic of Korea in 1971. He received his B.S., M.S., and Ph.D in Electrical Engineering from Seoul National University, in 1995, 1997, and 2008, respectively. He is currently a Senior Research Engineer in the Fuel Cell Vehicle Team 2 of Hyundai Motor Company, Republic of Korea. His main interest include the design and control of power electronic converters, inverters, and power system dynamics for fuel cell vehicles.

Jong-Hoon Kim received his B.S. in Electrical Engineering from Chungnam National University (CNU), Daejeon, Republic of Korea, in 2005 and is currently pursuing both his M.S. and Ph.D. at Seoul National University (SNU), Seoul, Republic of Korea. His research interests include battery management systems (BMS) and fuel cell systems. Mr. Kim is a Student Member of the IEEE and the Korean Institute of Power Electronics (KIPE).

Joung-Hu Park received his B.S., M.S., and Ph.D. from the Electrical Engineering and Computer Science Department of Seoul National University, Seoul, Republic of Korea in 1999, 2001 and 2006, respectively. He is currently an Assistant Professor at Soongsil University, Seoul, Republic of Korea. His interests include the analysis and design of high-frequency switching converters, driver circuits for PDP displays, and piezoelectric transformer power applications.

Bo-Hyung Cho received his B.S. and M.E. in Electrical Engineering from the California Institute of Technology, Pasadena, California. He received his Ph.D. also in Electrical Engineering, from Virginia Polytechnic Institute and State University (Virginia Tech), Blacksburg, Virginia. Prior to his research at Virginia Tech, he worked for two years as a Technical Staff Member in the Power Conversion Electronics Department of the TRW Defense and Space System Group. From 1982 to 1995, he was a Professor in the Department of Electrical Engineering at Virginia Tech. He joined the School of Electrical Engineering at Seoul National University, Seoul, Republic of Korea in 1995 and he is presently a Professor. His main research interests include power electronics, modeling, analysis and control of spacecraft power processing equipment, power systems for space stations and space platforms, and distributed power systems. Prof. Cho received the 1989 Presidential Young Investigator Award from the National Science Foundation. He is a Fellow of the IEEE Power Electronics Society, and a member of Tau Beta Pi.